

Raman scattering features of lead pyroantimonate compounds. Part I: XRD and Raman characterization of $\text{Pb}_2\text{Sb}_2\text{O}_7$ doped with tin and zinc

F. Rosi,^a V. Manuali,^a C. Miliani,^{a,b*} B. G. Brunetti,^a A. Sgamellotti,^{a,b} T. Grygar^c and D. Hradil^{c,d}

Yellow pyroantimonates Pb–Sb, Pb–Sb–Sn and Pb–Sb–Zn were synthesized by solid-state reactions at high temperature and characterized by X-ray diffraction and Raman spectroscopy. The lattice size of cubic pyrochlores increases with Sn and Zn doping and with Pb overstoichiometry, indicating the replacement of Sb^{5+} by the larger cations. This fact permits the understanding of the corresponding Raman spectral modifications as a consequence of the changes in the local symmetry of the Sb–O polyhedra, justifying the exploitation of Raman spectroscopy to noninvasively identify structural modifications of pyroantimonate pigments in artworks. Copyright © 2008 John Wiley & Sons, Ltd.

Keywords: XRD; Raman spectroscopy; cubic pyrochlores; lead antimonate yellow; Naples yellow

Introduction

Lead antimonate yellow ($\text{Pb}_2\text{Sb}_2\text{O}_7$) is one of the oldest known synthetic pigments, as its production goes back to at least 3500 years ago. It was employed as an opacifying and coloring agent in yellow glass in the Middle East artistic production from Egyptian, Mesopotamian, Babylonian and Assyrian workshops. In Western European art, lead antimonate has been used since the 16th century as yellow enamel pigment in Italian *majolica* and later in paintings replacing the lead–tin yellow and assuming the name *luteolum Napolitanum* (Naples yellow) as reported in a treatise by Andrea Pozzo in 1693–1700.^[1,2]

Naples yellow has a cubic pyrochlore structure, and it is the isostructural anhydrous analogue of the natural mineral bindheimite, $\text{Pb}_2\text{Sb}_2\text{O}_6(\text{O},\text{OH})$, which, however, was never employed as a pigment.^[1] A focus point of great interest was when in 1998 Roy and Berrie^[3] demonstrated through X-ray powder diffraction (XRD) and scanning electron microscopy-energy dispersive spectroscopy (SEM-EDS) the existence of a modified Naples yellow based on a ternary oxide of lead, antimony and tin ($\text{Pb}_2\text{Sb}_{2-x}\text{Sn}_x\text{O}_{7-x/2}$), whose use seemed to be restricted to Roman painters of the 17th century. Only recently the existence of the modified structure been confirmed, also suggesting that its use was not necessarily restricted to 17th century Roman artistic production. In particular, using micro-Raman spectroscopy Ruiz-Moreno *et al.*^[4] and Sandalinas *et al.*^[5] identified the ternary oxide in an Italian 17th century painting and a 16th century *majolica*, while using X-ray fluorescence (XRF) and XRD investigations Hradil *et al.*^[6] detected it in five Mid-European paintings from the 18th to 19th centuries.

The origin and use of lead antimonate yellows as a painting pigment is addressed in plenty by Renaissance ceramic production. In particular, regarding the modified Naples yellow it is worth reporting that Piccolpasso in *Li tre libri dell'arte del vasaio* (1557)

mentioned the practice of adding *tutia alessandrina* for obtaining a very particular orange-yellow shade of lead antimonate.^[7] *Tutia alessandrina* has been interpreted as tin oxide,^[8] but more likely refers to zinc oxides as indicated by a long series of quotations in occidental historical sources of the 17th century.^[2] Thus it is of interest to further investigate the occurrence of lead pyroantimonate and its modified structures in Italian *majolica* of the 16th century. For this reason, we have carried out a systematic study on lead antimonate compounds doped with tin or zinc cations, with the final objective of exploiting fiber-optic micro-Raman spectroscopy as a noninvasive routine analysis of Pb–Sb-based yellows in ceramic artworks. To this goal, reference pigments Pb–Sb–Sn, Pb–Sb–Zn and Pb–Sb (with different Pb : Sb stoichiometric ratios) were synthesized following historical recipes and then characterized by XRD with Rietveld refinement, obtaining the crystallographic structures and lattice parameters. The structural information was used to interpret the modification

* Correspondence to: C. Miliani, Istituto CNR-ISTM (Istituto di Scienza e Tecnologie Molecolari), c/o Dipartimento di Chimica, Università degli Studi di Perugia, Via Elce di Sotto 8, 06123 Perugia, Italy. E-mail: miliani@thch.unipg.it

a Centro di Eccellenza SMAArt (Scientific Methodologies applied to Archaeology and Art), c/o Dipartimento di Chimica, Università degli Studi di Perugia, Via Elce di Sotto 8, 06123 Perugia, Italy

b Istituto CNR-ISTM (Istituto di Scienza e Tecnologie Molecolari), c/o Dipartimento di Chimica, Università degli Studi di Perugia, Via Elce di Sotto 8, 06123 Perugia, Italy

c Institute of Inorganic Chemistry of the ASCR, v.v.i, 25068 Rez, Czech Republic

d Academy of Fine Arts in Prague, ALMA laboratory, U Akademie 4, Prague 7, Czech Republic

Table 1. Synthesis conditions and lattice parameter (*a*) of the cubic pyrochlores synthesized

Sample	Reagent	Molar ratio	Flux	Temperature (°C)	Lattice size of pyrochlore <i>a</i> (standard deviation in brackets) (Å)
PV_NY_25	Pb ₃ O ₄ , Sb ₂ O ₃	0.8 : 1 Pb : Sb	NaCl	900	10.394 (0.002)
PV_NY_26	Pb ₃ O ₄ , Sb ₂ O ₃	0.9 : 1 Pb : Sb	NaCl	900	10.407 (0.004)
PV_NY_27	Pb ₃ O ₄ , Sb ₂ O ₃	1 : 1 Pb : Sb	NaCl	900	10.418 (0.006)
PV_NY_28	Pb ₃ O ₄ , Sb ₂ O ₃	1.1 : 1 Pb : Sb	NaCl	900	10.424 (0.008)
PV_NY_29	Pb ₃ O ₄ , Sb ₂ O ₃	1.2 : 1 Pb : Sb	NaCl	900	10.416 (0.002)
PV_TY_1	Pb ₃ O ₄ , Sb ₂ O ₃ , SnO ₂	2 : 1.5 : 0.5 Pb : Sb : Sn	NaCl	800	10.567 (0.004); 10.478 (0.004)
PV_TY_60	PbCO ₃ , Sb ₂ S ₃ , SnO ₂	2.2 : 1.33 : 0.67 Pb : Sb : Sn	–	900	10.560 (0.002); 10.500 (0.002)
PV_TY_11	Pb ₃ O ₄ , Sb ₂ O ₃ , ZnO	2 : 1.5 : 0.5 Pb : Sb : Zn	NaCl	900	10.496 (0.002)

induced by Sn and Zn doping on Raman scattering signatures of the corresponding pyrochlore structures.

Experimental

The yellow pyroantimonates were synthesized by a solid-state reaction at high temperature ($T = 800\text{--}900^\circ\text{C}$) by adapting procedures reported in historical sources to laboratory conditions.^[1,2,6,8,9] Two different lead antimonates doped with tin (PV_TY_1 and PV_TY_60) were synthesized using Sb₂O₃ or Sb₂S₃, in order to evaluate the possible meaning of 'antimony' in historical recipes, which theoretically meant metallic, oxide and/or sulfide antimony. Moreover, the possible effect of the presence of lead carbonate instead of lead oxide as a starting material on the final structure was taken into account in PV_TY_60. A yellow antimonate doped with Zn (PV_TY_11) was obtained by adding ZnO to the raw material. Five unmodified Naples yellow pigments (PV_NY_25–29) were prepared at different Pb₃O₄ to Sb₂O₃ molar ratios (Pb : Sb from 0.8 : 1 to 1.2 : 1). Some syntheses were facilitated by an addition of a flux agent (10 wt% NaCl) according to the ancient recipes, where rock salt was mentioned. All reagents were of analytical grade (Sb₂S₃ was provided by Aldrich, PbCO₃ by PENTA, Czech Republic, and the remaining reagents by Lachema, Czech Republic) and used without further purification. The details of pigment syntheses are listed in Table 1, where reagents (type and molar ratio), fluxing agent and firing temperatures are also reported.

X-ray diffraction

For XRD analysis of synthetic pigments, a conventional powder diffractometer D5005 (Bruker) with Cu K α primary radiation was used. For the phase identification, X'Pert High-Score (PANalytical) with the 2005 release of PDF-2 database was used. The lattice size of the pyrochlore structures was refined using Rietveld code TOPAS 3.0 (Bruker AXS) with structural models taken from Inorganic Crystal Structure Database, Release 2007 (FIZ Karlsruhe, Germany).

Micro-Raman measurements

Micro-Raman measurements of synthetic pigments were performed with a laboratory JASCO Ventuno double-grating spectrophotometer equipped with a charge-coupled device (CCD) detector cooled to -50°C and coupled to an optical microscope. Raman spectra were excited using green radiation at 532.0 nm from a Nd : YAG laser. The laser power at the sample was always kept between 0.8 and 4 mW, the exposure time varied between 10 and 20 s with five accumulations and the resolution was about

1 cm⁻¹. Calibration of the spectrometer was accomplished using the Raman lines of a polystyrene standard.

Results and Discussion

Structure of lead pyroantimonate

Naples yellow (Pb₂Sb₂O₇) belongs to the class of cubic pyrochlore oxides whose general formula is A₂B₂O₇. The cubic pyrochlore structure (including the possible combinations A²⁺ and B⁵⁺ or A³⁺ and B⁴⁺) is common to a large group of compounds showing an amazing variety of chemical compositions and exploitable properties.^[10,11] The stability of such structure is mainly related to the cation radius ratio, with the A cation that must be appreciably larger than the B cation.^[12] It can be described as two interpenetrating networks as shown in Fig. 1. The B₂O₆ framework consists of corner-sharing BO₆ octahedra linked to hexagonal crowns, whose centers are filled with the A cations. The hexagonal crowns are in groups of four and the corresponding four A cations form a A₄O' tetrahedrons with an oxygen atom at its center (A₂O' network). All the B–O bonds are equivalent and each A atom is bonded to two kinds of oxygen atoms O and O' (belonging to the two different networks). The B₂O₆ network is structurally stable, with the A cations serving primarily for charge balance. In fact, the larger A cations occupying the large vacancies left in between the B–O lattice do not directly contribute to the cohesion of the pyrochlore three-dimensional lattice.

XRD characterization of synthesized lead pyroantimonate compounds

The synthesis products contained pyrochlores as major products according to XRD and Rietveld analysis. In Pb-excess lead antimonates, trace of an unidentified phase was observed (no PDF item fit the admixtures). The most intense diffraction lines of these admixtures were always less than 10% of the most intense diffraction line of pyrochlores except for the sample with the largest Pb excess. XRD patterns of modified lead antimonate PV_TY_60, 1 and 11, synthesized with the addition of SnO₂ or ZnO to the raw salt, confirmed the formation of cubic pyrochlore structures with larger cell sizes with respect to that of the binary Sb–Pb yellow (synthetic Pb₂Sb₂O₇, card number 1-74-1354, $a = 10.4000\text{ \AA}$), as reported in Table 1. A trace of unreacted SnO₂ was found in Sn-containing pyrochlore specimens, but the lattice sizes of both pyrochlores indicate clearly that a substantial portion of Sn⁴⁺ entered the pyrochlore lattice. The synthesis of Pb–Sb–Sn yellow from Sb₂S₃ (PV_TY_60) did not require NaCl flux, and XRD results revealed the

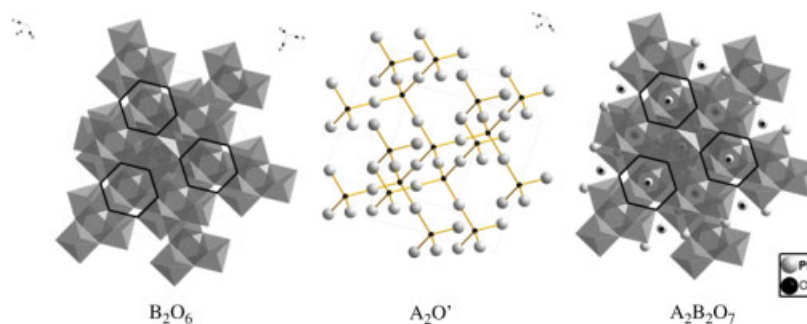


Figure 1. The ideal crystal structure of pyrochlore represented as two interpenetrating networks. Gray octahedra contain B cations (for lead antimonate it corresponds to Sb) with oxygen atoms located at the six vertices; white spheres denote A cations (for lead antimonate it corresponds to Pb); and black spheres represent oxygen anions. The A_2O' network corresponds to a four-coordinate O' ions and two-coordinate A cations. The B_2O_6 framework consists of BO_6 octahedra sharing all vertices to form large cavities. The structures are interwoven such that the O' ions of the A_2O' network occupy the centers of these cavities, while the A cations reside in puckered hexagons formed by oxygen atoms in the B_2O_6 framework. The final coordination number of the A cations is 8, including the two oxygen atoms in the A_2O' network that cap the puckered hexagonal ring above and below. This figure is available in colour online at www.interscience.wiley.com/journal/jrs.

presence of 12% of lanarkite (Pb_2OSO_4) in the final product. The lattice sizes of Sn-substituted lead antimonates are in good agreement with the database items ($Pb_2SbSnO_{6.5}$, card number 39–928, $a = 10.5645 \text{ \AA}$), and the lattice size of Zn-doped specimens also increased significantly. Such increase of the cell parameter due to incorporation of larger cations is in line with published data.^[13] This confirms that Sn and Zn have both entered octahedral sites, thereby causing deformation of the local symmetry of the ideal pyrochlore structure. The small expansion in the average cubic pyrochlore unit cell dimension can be interpreted on the basis of ionic size considerations; indeed, the octahedral coordination cation radius increases in the order $Sb^{5+} < Sn^{4+} < Zn^{2+}$.^[14–16]

An XRD study also revealed the presence of a bimodality in the lattice size of the Pb–Sb–Sn (lattice parameters a are $10.55–10.56 \text{ \AA}$ and $10.46–10.50 \text{ \AA}$) as already reported in a previous work,^[6] where it is stated that the same bimodality was also present in original Pb–Sb–Sn pigments from paintings, proving that it was not a specific drawback of the adopted synthesis route but rather a tendency of element demixing in a given composition. It is possible that other real historical specimens of lead pyroantimonates also have more complex mineral compositions because the exact stoichiometry of the raw materials was hardly guaranteed in the resulting pigment.

The product color was yellow in all reported cases, with a purer yellow hue in the case of Sn-containing specimens, an orange hue in the Zn-containing specimen and a darker yellow hue in the case of pure lead antimonates with a Pb : Sb ratio exceeding 1.

Vibrational characterization of synthesized lead pyroantimonate compounds

Theoretical analysis provided the identification for cubic pyrochlore structure of 26 normal modes; among them six are Raman active, namely, A_{1g} , E_g and $4F_{2g}$. From the symmetry coordinates, the Raman active phonons depend on the oxygen vibration only.^[17] Hence, it is expected that their values should be nearly the same for oxide pyrochlores in the cubic structure, and slight differences in the Raman wavenumbers can occur because of the differences in the nature of A and B cations. On the basis of these considerations, the large Raman literature on general cubic pyrochlore structure is considered here for the interpretation of the scattering features of lead antimonate yellow pigments. The spectrum reported in Fig. 2 has been collected from an unmodified

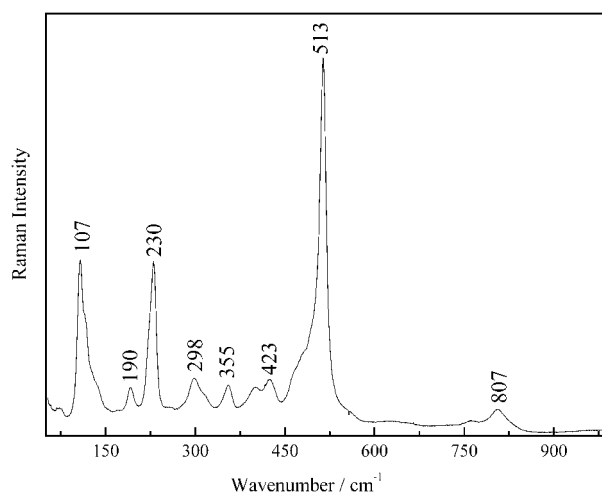


Figure 2. Micro-Raman spectrum collected from the sample PV_NY_25.

lead antimonate yellow (named PV_NY_25, Table 1), for which XRD analysis showed a single-phase cubic pyrochlore structure with the lattice parameter a of 10.394 \AA . On observing the spectrum, it is clear that the number of vibrational bands observed is larger than that predicted by factor group analysis. The additional bands are more likely related to a disorder-induced symmetry lowering due to distortion of the SbO_6 octahedra or displacements of the Pb cations.^[18,19] The fact that the XRD analysis yielded a well-defined pyrochlore structure, while the vibrational spectrum did not agree with the factor group prediction, is because XRD typically gives information on an average structure, whereas Raman spectroscopy is sensitive to the local balance among the interatomic forces.

The most intense scattering peak at about 510 cm^{-1} can be ascribed to the A_{1g} mode and corresponds to the totally symmetric elongation of the SbO_6 octahedra. At lower wavenumbers, there are two overlapping modes that could be attributed to vibrational modes related to Sb–O and Pb–O bonds, E_g at around 350 cm^{-1} and F_{2g} at around 300 cm^{-1} .^[20] In the lower spectral range ($100–300 \text{ cm}^{-1}$), the vibrations of Pb_4O tetrahedra are expected in terms of the lattice vibration of the Pb cation^[21] and vibration of the Pb cation with respect to the Sb–O sublattice.

The band observed at higher wavenumber (about 800 cm^{-1}) does not have an unequivocal assignment: some authors report

that it is an overtone or combination band, or an F_{2g} mode.^[22,23] Vandenberg *et al.*^[18] found a band at about 700 cm^{-1} in titanate cubic pyrochlore and assigned it to a distortion of the octahedra BO_6 or displacement of atoms changing the structure and the degree of symmetry.

Influence of Zn and Sn substitution in lead antimonate

Deformation of the pyrochlore structure due to the introduction of the third cation strongly affects the Raman scattering features, as is obvious in Fig. 3, where a comparison of the spectrum of binary Pb–Sb compound (PV_NY_25) with those of Sn- and Zn-modified yellows (PV_TY_11, PV_TY_1 and PV_TY_60) is presented.

First, the most important modifications are the collapse of the intense band at 510 cm^{-1} (A_{1g} mode) and the appearance of a well-resolved band at about 450 cm^{-1} , which is particularly evident for the Zn-containing sample. The Sb–O bonds of the octahedral network, being more rigid and relatively covalent, are very sensitive to any variation in the pyrochlore structure, reflecting strong changes in the range of the Sb–O stretching mode ($500\text{--}400\text{ cm}^{-1}$). A similar spectral modification has already been observed by Vandenberg *et al.*^[18] while studying the relative stability of rare-earth stannate pyrochlores, $\text{A}_2\text{Sn}_2\text{O}_7$, till a borderline structure for which they observed an evident diminishing of the band at about 500 cm^{-1} and its splitting into two peaks ascribed to A_{1g} and F_{2g} modes.

Secondly, the Pb–O lattice mode at 110 cm^{-1} shifts towards higher wavenumbers in the samples doped with Zn and Sn. The larger shift is for Zn-modified Naples yellow in which the Pb–O lattice mode is positioned at 145 cm^{-1} . In the case of Sn-modified Naples yellow PV_TY_1, the Pb–O mode appears as a sharp doublet at 125 and 142 cm^{-1} (Fig. 3). Third, with respect to binary lead antimonate yellows, the ternary compounds show a clear increase of a band at about 330 cm^{-1} (Sb–O and Pb–O modes); also in this case, this feature is more intense for the Zn-containing sample. Finally, the unassigned signal at a higher wavenumber, which lies at 810 cm^{-1} in the binary Pb–Sb compound, is red-shifted to 775 in Pb–Sb–Sn and to 721 cm^{-1} in the Pb–Sb–Zn ternary oxide.

The ternary Pb–Sb–Sn compound PV_TY_60, synthesized starting from PbCO_3 and antimony sulfide, shows further

peculiarities: the intense band at about 200 cm^{-1} is absent and new bands at about 970 , 1055 and 1077 cm^{-1} are observed. These last features, better shown in the inset of Fig. 3, can be ascribed to lead sulfates (lanarkite, Pb_2OSO_4)^[24] detected also by XRD and formed as by-products in the synthesis starting from antimony sulfide.^[6]

Influence of Pb–Sb stoichiometry in lead antimonate

Regarding samples of Naples yellow synthesized with Pb:Sb reagent molar ratio ranging from 0.8:1 to 1.2:1, XRD analysis showed the formation of major pyrochlore structures with the lattice parameter a slightly increasing on increasing Pb:Sb overstoichiometry, as reported in Table 1. Conversely, the variation in the reagent stoichiometry causes evident modification in the low wavenumber part of the Raman spectrum (Fig. 4). In particular, the wavenumber of the Pb–O lattice mode at about 110 cm^{-1} is shifted to a higher value (120 cm^{-1}) and becomes broad with the increase of Pb:Sb ratio. The intense A_{1g} signal at 510 cm^{-1} is strongly modified only in the sample synthesized with the largest amount of Pb_3O_4 (PV_NY_29, Pb:Sb = 1.2:1), in which it decreases and new evident features appear at 460 and 490 cm^{-1} . Also the Raman peaks at 320 and 655 cm^{-1} get stronger in Pb-excess compounds. All these spectral modifications are similar to what was previously described for Naples yellow doped with Sn and Zn, suggesting that here also a third cation could have entered into the pyrochlore structure. Literature data reported that during the synthesis of different pyrochlores (among them also lead antimonates) an excess of Pb can be accommodated as Pb^{4+} in the B-sites.^[25–27] Considering this and the Raman spectral modifications, it can be suggested that for Naples yellow also a Pb-excess could lead to the formation of a structure with symmetry resembling that of ternary pyrochlores, as Sb^{5+} cations are partially substituted by the larger Pb^{4+} (ionic radius in octahedral coordination 0.78 \AA)^[14].

Conclusion

Modified lead antimonate yellows were prepared by solid-state synthesis adapted from ancient recipes by adding SnO_2 , ZnO or in the presence of a Pb overstoichiometry. XRD structural

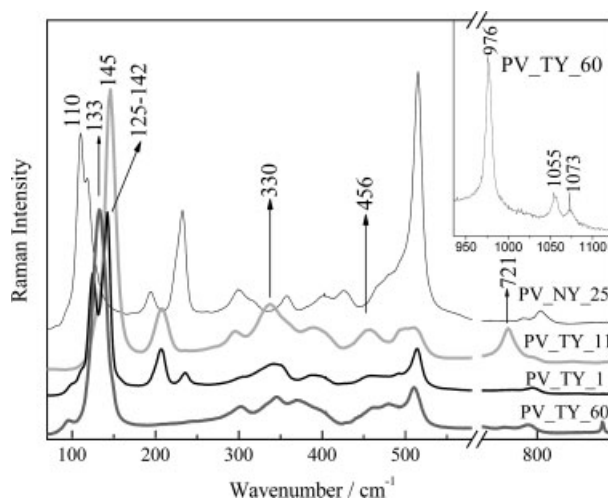


Figure 3. Comparison among the micro-Raman spectra collected from lead antimonate in binary composition (PV_NY_25) and ternary composition with Sn (PV_TY_1 and PV_TY_60) and Zn (PV_TY_11); in the inset, the enlarged range at higher wavenumbers is reported for sample PV_TY_60.

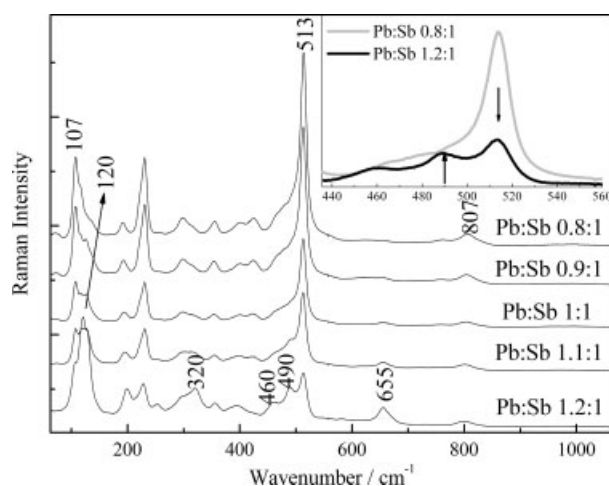


Figure 4. Micro-Raman spectra collected from the lead antimonate compounds in binary composition with varying Pb:Sb molar ratio. Inset: an enlarged view of the A_{1g} mode in the spectra with minimum (gray line) and maximum (black line) Pb content normalized at 110 cm^{-1} .

analysis confirmed that all the synthesized compounds have a well-defined cubic pyrochlore structure, and the doping affects only the average cubic pyrochlore unit cell dimension which is significantly increased with the replacement of some Sb^{5+} with the larger cations Sn^{4+} , Zn^{2+} and probably Pb^{4+} .

Conversely, the Raman spectra turned out to be very sensitive to local order or disorder and by the local geometry of both the polyhedra AO_8 and BO_6 modified by substitution of Sb in the B-site. Indeed, differently from XRD, where disorder is observed as an average of the scattering factors, the vibrational spectra are affected not only by the atomic species distribution but also by the different interatomic interactions.^[28] For this reason, the assignment of vibrational spectra of disordered pyrochlore can be arduous; nevertheless, this study provided information to be used for the interpretation on Raman spectra of modified lead antimonate yellow from real artworks. The Pb–O stretching mode of the $\text{A}_2\text{O}'$ lattice proved to be very sensitive to any small distortion of the pyrochlore structure. In the compounds synthesized in this work, it shifts from 110 cm^{-1} for the unmodified lead antimonate to 145 cm^{-1} for the pigment doped with zinc, or appearing as a doublet (124 and 142 cm^{-1}) for the salt doped with tin. Sandalinas *et al.*^[5] found a similar trend but with different values in lead antimonate yellow doped with tin (137 cm^{-1}) and silicon (132 cm^{-1}). On the other hand, the wavenumber reported for the Pb–O lattice mode of unmodified Naples yellow inherently varies from 125 cm^{-1} ^[29] to $130\text{--}147\text{ cm}^{-1}$,^[21,30] and it has been proved to be also affected by the firing temperature used to obtain the pigment.^[29] As a consequence, the Pb–O vibration cannot be considered for discriminating the different lead antimonate yellows in binary and ternary compositions and in nonstoichiometric Pb : Sb molar ratios.

The A_{1g} mode at 510 cm^{-1} , corresponding to the totally symmetric elongation of the SbO_6 octahedra, is less affected by small variation of the unmodified structure but suddenly collapses and shows a shoulder at about 450 cm^{-1} when some Sb^{5+} is replaced with Sn^{4+} or Zn^{2+} , suggesting the formation of a less stable pyrochlore structure as reported for rare-earth stannate pyrochlores of the $\text{A}_2\text{Sn}_2\text{O}_7$ series.^[18] This additional band appeared in a different position and with a different shape in the diverse ternary yellows (Sn or Zn containing), which also allow distinguishing the nature of the third oxide. Interestingly, similar spectral features are present in the Raman spectra reported by other authors^[4,5] on ternary Pb–Sb–Sn laboratory samples and ancient real ceramics and paintings; in these cases also, the band at 510 cm^{-1} is constrained and has a shoulder at 450 cm^{-1} .

Moreover, Raman investigations have allowed us to discriminate between the different starting materials in the recipes by detecting the presence of lead sulfates as by-products of the synthesis carried out with Sb_2S_3 . The presence of a binary lead antimonate compound with a Pb excess could be detected by the presence of a band at 650 cm^{-1} , which is specific to a nonstoichiometric Pb : Sb molar ratio.

In conclusion, the high sensitivity of Raman spectroscopy can be used for the analysis of particular varieties of lead antimonate yellows. The availability of a fiber-optic portable spectrometer allowed us to apply the knowledge acquired from laboratory synthesized compounds for the interpretation of spectra collected from lead–antimony yellow pigments of Renaissance *majolica* directly in museums. The data will be discussed in the part II of this paper.

Acknowledgements

This work was partially developed within the activities of the EU-ARTECH project (RII3-CT-2004-506171) of the 6th FP of the European Union. A partial support by MIUR (*Ministero dell'Istruzione, dell'Universita' e della Ricerca*) through the project FIRB 2003 (RBNE03SML9) is also acknowledged. The work in IIC ASCR was funded by research grant AV0Z4032918 and by Czech Science Foundation project 203/07/1324. The authors wish to thank Antonin Petrina (IIC ASCR, Rez, Czech Republic) who kindly performed XRD measurements and Claudio Seccaroni for helpful discussion on the history and use of lead antimonate pigments.

References

- [1] N. M. Wainwright, J. M. Taylor, R. D. Harley, in *Artists' Pigments: A Handbook of their History and Characteristics*, vol. 1 (Ed.: R. L. Feller), National Gallery of Art: Washington DC, USA, **1986**, pp 219.
- [2] C. Seccaroni, *Giallorino: storia dei pigmenti gialli di natura sintetica*, De Luca Editori D'Arte: Rome, **2006**.
- [3] A. Roy, B. H. Berrie, in *A New Lead-based Yellow in the Seventeenth Century, Painting Techniques History, Materials and Studio Practice*, (Eds.: A. Roy, P. Smith), The International Institute for Conservation of Historic and Artistic Works: London, **1998**, pp 160.
- [4] S. Ruiz-Moreno, R. Pérez-Pueyo, A. Gabaldón, M. J. Soneira, C. Sandalinas, *J. Cult. Herit.* **2003**, *4*, 309.
- [5] C. Sandalinas, S. Ruiz-Moreno, A. Lopez-Gil, J. Miralles, *J. Raman Spectrosc.* **2006**, *37*, 1146.
- [6] D. Hradil, T. Grygar, J. Hradilová, P. Bezdička, V. Grunwaldová, I. Fogaš, C. Miliani, *J. Cult. Herit.* **2007**, *8*, 377.
- [7] C. Piccolpasso, in *I Tre Libri dell'Arte del Vasaio*, All'Insegna del Giglio, Florence, **1976**.
- [8] J. Dik, E. Hermens, R. Peschar, H. Schenk, *Archaeometry* **2005**, *47*, 593.
- [9] E. Eastaugh, V. Walsh, T. Chaplin, R. Siddall, *Pigment compendium, A Dictionary of Historical Pigments*, Elsevier: Oxford, **2004**, pp 220–273.
- [10] B. J. Wuensch, K. W. Eberman, C. Heremans, E. M. Ku, P. Onnerud, E. ME. Yeo, S. M. Haile, J. K. Stalick, J. D. Jorgensen, *Solid State Ionics* **2000**, *129*, 111.
- [11] M. Pirzada, R. W. Grimes, J. F. Maguire, *Solid State Ionics* **2003**, *161*, 81.
- [12] T. A. Vanderah, I. Levin, M. W. Lufaso, *Eur. J. Inorg. Chem.* **2005**, *14*, 2895.
- [13] K. Sreedhar, A. Mitra, *J. Am. Ceram. Soc.* **2000**, *83*, 418.
- [14] J. E. Huheey, in *Chimica Inorganica*, Piccin, Padova, **1972**, pp 74.
- [15] S. Hati, D. Datta, *J. Phys. Chem.* **1996**, *100*, 4828.
- [16] V. Dimitrov, T. Komatsu, *J. Solid State Chem.* **2002**, *163*, 100.
- [17] H. C. Gupta, S. Brown, N. Rani, V. B. Gohel, *Int. J. Inorg. Mater.* **2001**, *3*, 983.
- [18] M. T. Vandenborre, E. Husson, J. P. Chatry, D. Michel, *J. Raman Spectrosc.* **1983**, *14*, 63.
- [19] E. A. Oliveira, I. Guedes, A. P. Ayala, J.-Y. Gesland, J. Ellena, R. L. Moreira, M. Grimsditch, *J. Solid State Chem.* **2004**, *177*, 2943.
- [20] M. T. Vandenborre, E. Husson, *J. Solid State Chem.* **1983**, *50*, 362.
- [21] R. J. H. Clark, L. Cridland, B. M. Kariuki, K. D. M. Harris, R. Withnall, *J. Chem. Soc., Dalton Trans.* **1995**, *16*, 2577.
- [22] M. Glerup, O. Faurkov Nielsen, F. Willy Poulsen, *J. Solid State Chem.* **2001**, *160*, 25.
- [23] S. Brown, H. C. Gupta, J. A. Alonso, M. J. Martinez-Lope, *J. Raman Spectrosc.* **2003**, *34*, 240.
- [24] Y. Batonneau, C. Brémar, J. Laureyns, J. C. Merlin, *J. Raman Spectrosc.* **2000**, *31*, 1113.
- [25] G. Burchard, W. Rüdorff, *Z. Anorg. Allg. Chem.* **1978**, *447*, 149.
- [26] R. A. Beyerlein, H. S. Horowitz, J. M. Longo, *J. Solid State Chem.* **1988**, *72*, 2.
- [27] K. Sreedhar, A. Mitra, *J. Am. Ceram. Soc.* **1999**, *82*, 1070.
- [28] A. P. Ayala, C. W. A. Paschoal, I. Guedes, W. Paraguassu, P. T. C. Freire, J. Mendes Filho, *Phys. Rev. B* **2002**, *66*, 214105–214105.
- [29] K. Sakellariou, C. Miliani, A. Morresi, M. Ombelli, *J. Raman Spectrosc.* **2004**, *35*, 61.
- [30] Ph. Colomban, G. Sagon, X. Faurel, *J. Raman Spectrosc.* **2001**, *32*, 351.